

BioVFM-21M: Benchmarking and Scaling Self-Supervised Vision Foundation Models for Biomedical Image Analysis

Jiarun Liu^{1,2,3}, Hong-Yu Zhou, Weijian Huang^{1,2,3}, Hao Yang^{1,2,3}, Dongning Song^{1,2,3}, Tao Tan⁴, Yong Liang³, and Shanshan Wang¹ (✉)

- ¹ Paul C. Lauterbur Research Center for Biomedical Imaging, Shenzhen Institutes of Advanced Technology, Chinese Academy of Sciences, Shenzhen, China
ss.wang@siat.ac.cn
- ² Pengcheng Laboratory, Shenzhen, China
- ³ University of Chinese Academy of Sciences, Beijing, China
- ⁴ Faculty of Applied Sciences, Macao Polytechnic University, Macao, China

Abstract. Scaling up model and data size have demonstrated impressive performance improvement over a wide range of tasks. Despite extensive studies on scaling behaviors for general-purpose tasks, medical images exhibit substantial differences from natural data. It remains unclear the key factors in developing medical vision foundation models at scale due to the absence of an extensive understanding of scaling behavior in the medical domain. In this paper, we explored the scaling behavior across model sizes, training algorithms, data sizes, and imaging modalities in developing scalable medical vision foundation models by self-supervised learning. To support scalable pretraining, we introduce BioVFM-21M, a large-scale biomedical image dataset encompassing a wide range of biomedical image modalities and anatomies. We observed that scaling up does provide benefits but varies across tasks. Additional analysis reveals several factors correlated with scaling benefits. Finally, we propose BioVFM, a large-scale medical vision foundation model pre-trained on 21 million biomedical images, which outperforms the previous state-of-the-art foundation models across 12 medical benchmarks. Our results highlight that while scaling up is beneficial for pursuing better performance, task characteristics, data diversity, pretraining methods, and computational efficiency remain critical considerations for developing scalable medical foundation models.

Keywords: Foundation models · Large medical dataset · Benchmarking · Correlation analysis · Scaling law · Self-supervised learning.

1 Introduction

Biomedical imaging is at the forefront of healthcare, playing an essential role in the diagnosis and treatment of diseases [2,23]. Foundation models (FMs) offer a more efficient alternative that allows straightforward application to a wide range

of tasks with minimal labeled data [28,2]. The success of FMs is largely driven by the scalable self-supervised approaches [18,6], which enable generalizable representations from large datasets without annotations [24]. The well-known scaling law [11,7] implies that the model performance can be continuously improved with increased model size, data size, and amount of computes. However, training large foundation models is expensive [5] – in computation, energy, time, and data. Unfortunately, most of the existing scaling studies are drawn from the general domain [11,7,5,1,26], while biomedical data exhibit distinct characteristics compared to general data [13,31]. Considering the diminishing returns and substantial resource requirements [7], it is important to understand the scalability in the medical domain before further scaling up.

Nevertheless, large-scale scalability research in biomedicine requires sufficient training data [11]. Despite the superior performance, many existing medical FMs and datasets are developed with a focus on a specific modality [20,30,32,8,9,22], organ [33,14], or task [15,3]. Such a focus, by its nature, maintains the existing dataset biases [10] that are limited to specific biomedical domains and reduces the opportunities to combine more data from diverse modalities [17], thus limiting the diversity and quantity of training data. The model may struggle to learn generalizable representations across different modalities and anatomical structures [17], which limits the applicability of learned scaling behavior to a wider spectrum of medical applications.

In this work, we explore the scaling behavior for developing self-supervised medical vision FMs. Our empirical experiments reveal that scaling up did take benefits but differed across tasks, whereby optimal scaling strategy depends on task and dataset characteristics. Our contributions are summarized as follows:

- We curate BioVFM-21M, a large biomedical image dataset with over 21 million images, spanning 10 imaging modalities and 30 anatomical structures.
- We conducted extensive experiments with an additional correlation analysis in exploring the scalability across model sizes, training algorithms, data sizes, and imaging modalities in developing self-supervised medical vision FMs.
- We propose BioVFM, a self-supervised medical vision foundation model at scale, demonstrating remarkable performance across 12 medical benchmarks.

2 The BioVFM-21M dataset

To support the training of BioVFM, we curated BioVFM-21M, a large biomedical image dataset consisting of 21 million biomedical images from over 43 publicly available data sources. BioVFM-21M following three key principles: 1) *large-scale*: As shown in Fig. 1b, BioVFM-21M is composed of 21 million images, which is significantly larger than previous datasets sourced from medical image datasets or medical websites. 2) *data diversity*: As illustrated in Fig. 1a and 1c, BioVFM-21M cover most of the major anatomical regions of the human body from microcosmic to macroscopic across 10 biomedical imaging modalities, including CT, MR, Microscopy, X-Ray, Dermoscopy, Ultrasound, Endoscopy, Fun-

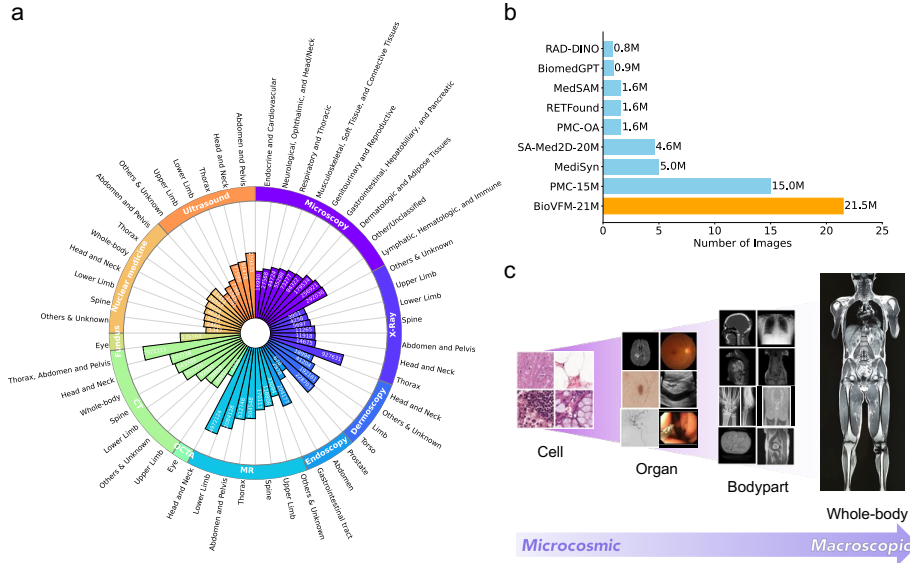


Fig. 1. The proposed BioVFM-21M dataset. **a.** BioVFM-21M covers a wide range of imaging modalities and anatomical areas. The illustration is exponential-scaled. **b.** Comparison with existing large-scale biomedical image datasets. **c.** BioVFM-21M covers images from microcosmic to macroscopic.

us, Nuclear medicine, and OCTA. 3) *publicly available*: We focused on collecting data from publicly available sources to ensure transparency and accessibility. We will open the links of source datasets, processing codes, and more details of BioVFM-21M in <https://github.com/JiarunLiu/BioVFM-21M>.

To reduce the risk of data leakage, we excluded 1.8 million testing and validation images based on default data splits of each source dataset. In addition, all data sources related to our evaluation benchmarks were excluded from BioVFM-21M, ensuring that performance is not inflated by overlapped training and evaluation data. For 3D images, we slice them along axial, sagittal, and coronal views. The initial version of our dataset has over 30 million images, while all of the detected padding slices were removed since it does not have anatomical structure information. Furthermore, we removed images with aspect ratio smaller than 0.4. All images were normalized to 0-255 and resized to 224x224px while preserving their original aspect ratio.

3 Method

3.1 Self-supervised pretraining

We investigate the scalability of the self-supervised medical vision foundation models by varying model sizes, training algorithms, data numbers, and imag-

ing modalities. Specifically, we select two representative self-supervised learning methods for model and algorithm scalability experiments: MAE [6] (BioVFM-M) and DINO V2 [18] (BioVFM-D). These methods are trained with model sizes ranging from 5 million to 303 million parameters while other settings follow the default settings as the author suggests. To optimize computational resources, we pretrain these models on a subset of 2.45 million images drawn from diverse imaging modalities and anatomical structures, sourced from [12,16]. In the data and modality scaling experiments, we extract two smaller subsets from BioVFM-21M with different data numbers and image modalities, which are BioVFM-US and BioVFM-0.2M. The BioVFM-US is an ultrasound subset with 0.4 million ultrasound images from BioVFM-21M. Similarly, BioVFM-0.2M is another small subset that was randomly sampled from BioVFM-21M but contains all 10 image modalities from BioVFM-21M. We train three models with 303 million parameters using BioVFM-D on BioVFM-US, BioVFM-0.2M, and the full BioVFM-21M dataset. All models are pretrained on a server with 8 NVIDIA A100 80GB GPUs.

3.2 Evaluation benchmarks

In contrast to previous scaling studies that evaluate loss values, we assess model performance using the Area Under the Curve (AUC) score across 12 diagnostic benchmarks from MedMNIST [25]. The 12 benchmarks span a variety of imaging modalities, anatomical regions, number of classes (ranging from 2 to 14), sample numbers (from 100 to 100,000), and task types (binary/multi-class classification, multi-label classification). For evaluation, we finetune the pretrained models using linear-probing settings with an NVIDIA 2080Ti GPU by default. We specify the learning rate by 0.01 with AdamW optimizer, a batch size of 128. The maximum epoch number is 100 and early stopping is applied based on validation loss. These hyperparameters were chosen based on preliminary experiments, which demonstrated optimal performance. In addition, we compare the performance of BioVFM with ImageNet pretrained ViTs (IN21K-ViT-Base, IN21K-ViT-Large), RAD-DINO [20], BiomedCLIP [29], and BiomedGPT [29], which differ in pre-training data size (0.9 to 21 million), supervision (self-supervised learning (SSL), supervised learning (SL), vision-language pretraining (VLP)), model size (85.8 to 303 million), and data sources (natural or medical data).

3.3 Scalability analysis

To quantify the benefits of model scaling, we fit a power function $y = e^b x^a$ as proposed in [21]. Here a indicates the slope of the scaling curve and b is the corresponding intersection. A higher slope a indicates that scaling up the model size has a more positive effect on performance for the corresponding task. Additionally, to investigate the underlying factors related to scalability, we extract 4 quantitative metrics from downstream tasks: the number of samples, Davies-Bouldin Index (DBI) [4], the number of classes, and g-zip compressibility [19]. The number of samples and the number of classes provide fundamental insights

Table 1. Average performance on 12 MedMNIST benchmarks. The values in brackets indicate 95% CI. †: Developed with classification labels. ‡: Developed with image-text pairs. *: Developed for a specific medical domain. MCC: Matthews Correlation Coefficient. BA: Balanced Accuracy.

Model	MCC	BA	F1	AUC
IN21K-ViT-Base [†]	61.59 (59.98,62.97)	69.46 (68.53,70.35)	67.16 (66.39,67.86)	91.86 (91.18,92.43)
IN21K-ViT-Large [†]	63.33 (61.78,64.73)	70.87 (69.83,71.80)	67.79 (66.97,68.54)	92.26 (91.52,92.85)
RAD-DINO[20] [*]	62.88 (61.38,64.26)	69.43 (68.50,70.32)	67.07 (66.33,67.77)	91.49 (90.65,92.21)
BiomedGPT[27] [‡]	64.71 (63.25,66.04)	71.92 (71.01,72.81)	68.63 (67.85,69.42)	92.86 (92.23,93.46)
BiomedCLIP[29] [‡]	66.60 (65.19,67.86)	73.24 (72.36,74.15)	71.29 (70.56,72.01)	93.52 (92.95,94.00)
BioVFM	69.92 (68.52,71.12)	76.05 (75.09,76.92)	73.43 (72.55,74.25)	94.40 (93.90,94.84)

into the dataset’s characteristics, while DBI reflects the complexity of data distribution and classification difficulty. The g-zip compressibility, on the other hand, quantifies the information redundancy of the data. With these metrics, we analyze the correlation between the computed values and the scaling slopes a using the Pearson Correlation Coefficient (PCC) in Sec. 4.5.

4 Results

4.1 BioVFM: Biomedical vision foundation model at scale

Based on the BioVFM-21M dataset, we propose BioVFM, a Biomedical Vision Foundation Model at scale. By pretraining on 21 million biomedical images with 630 million parameters using BioVFM-D, BioVFM sets a new benchmark for generalizable medical foundation models. As shown in Table 1, BioVFM significantly outperforms existing medical foundation model BiomedGPT [27], BiomedCLIP [29], and RAD-DINO [20] across 12 medical benchmarks with linear-probing by at least 3.32% in MCC, 2.81% in BA, 2.14% in F1 score, and 0.94% in AUC. Our results highlight the advantages of scalable self-supervised pretraining in the development of generalizable medical foundation models.

4.2 Model scaling

As shown in Fig. 2a and Fig. 3, when scaling up the model size from 5 to 303 million, both BioVFM-D and BioVFM-M demonstrate improved mean AUC as the scaling law predicted. The average performance of BioVFM-D was improved by

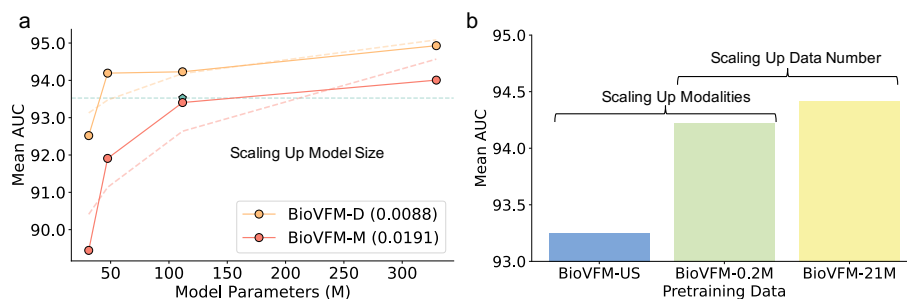


Fig. 2. Medical FMs scales with model size, data size, and number of modalities. **a.** Model scaling of BioVFM-D and BioVFM-M. The dotted line indicates the fitted scaling curves and the value within brackets indicates the slope a . The turquoise star indicates the performance of BiomedCLIP. **b.** Data and modality scaling with BioVFM-D. The results are averaged over 12 medical benchmarks.

2.1% and BioVFM-M was improved by 2.3% through scaling up model size. However, scaling up model size does not guarantee consistent improvements across all medical tasks. As shown in Fig. 4, the scaling slope across different tasks and imaging modalities shows considerable variation, with differences exceeding 40-fold. For example, increasing model size from 5.5 to 303.3 million improves AUC by 4.65% on ChestMNIST, whereas performance plateaus on RetinaMNIST when model sizes beyond 21.7 million parameters.

Interestingly, we observe a similar trend in the relative scaling slopes across different evaluation benchmarks. Specifically, for each benchmark, the computed scaling slopes may vary, but the relative order of the slopes remains stable: the top 5 benchmarks with higher slopes consistently exhibit greater scaling benefits compared to those with lower slopes, regardless of the pretraining method used. The gap between high and low slope groups ranges from 3 to 14 folds, highlighting significant variability in scaling efficiency. However, estimating scaling benefits based on qualitative factors, such as imaging modality, anatomy, or view orientation, remains challenging. For instance, although ChestMNIST and PneumoniaMNIST share the same imaging modality and anatomical region, they show different scaling slopes. OrganAMNIST, OrganCMNIST, and OrganSMNIST are derived from the same CT data but in different views, they demonstrate similar scaling slopes across all three tasks. These findings suggest that more nuanced factors, such as dataset size, task complexity, and intra-class variability, are likely to influence the scalability of vision foundation models.

4.3 Data and modality scaling

As shown in Fig. 2b, scaling up image modalities leads to a noticeable improvement of 0.97% in the mean AUC across 12 medical diagnosis tasks, demonstrating the importance of data diversity for enhancing generalizability. Surprisingly, we found that improving performance by scaling imaging modalities does

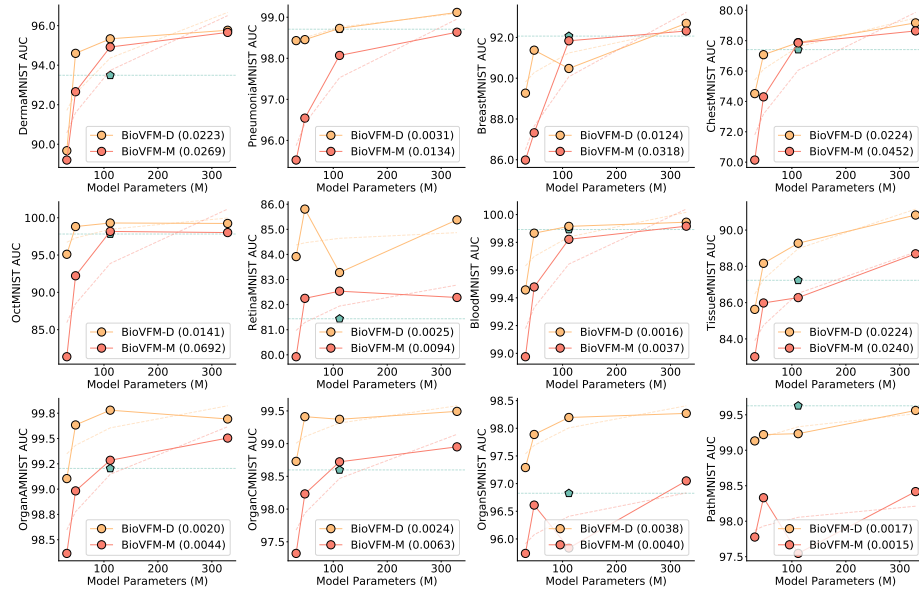


Fig. 3. Model scaling results across 12 medical benchmarks. The dotted line indicates the fitted scaling curves and the value within brackets indicates the slope a . The turquoise star indicates the performance of BiomedCLIP.

not necessarily degrade the performance of specific tasks. The model trained on BioVFM-0.2M outperforms the model trained on BioVFM-US on the ultrasound benchmark (92.75% vs. 91.87% in AUC). Furthermore, simply scaling up the data size can yield diminishing returns, with only a 0.2% improvement in mean AUC despite a 100-fold increase in data size. These findings suggest that data diversity, rather than just data size, plays a more significant role in developing scalable and generalizable medical foundation models.

4.4 Scalability vary across pretraining algorithms

We compare the self-supervised pretraining algorithms by two dimensions: the scaling efficiency (quantified by scaling slope) and the performance on medical benchmarks. As shown in Fig. 2a, BioVFM-M exhibits a steeper scaling slope (0.0191) compared to BioVFM-D (0.0088), suggesting it benefits more from increased model capacity. However, as shown in Fig. 3, BioVFM-D outperforms BioVFM-M in almost all the benchmarks. The average gap between BioVFM-D and BioVFM-M across all benchmarks and model sizes is 1.7%. Notably, BioVFM-D outperforms BiomedCLIP on 7 out of 12 tasks even when using $3.5\times$ fewer parameters. This divergence underscores the critical role of pertaining objective design in determining both scalability and downstream task performance when developing medical foundation models.

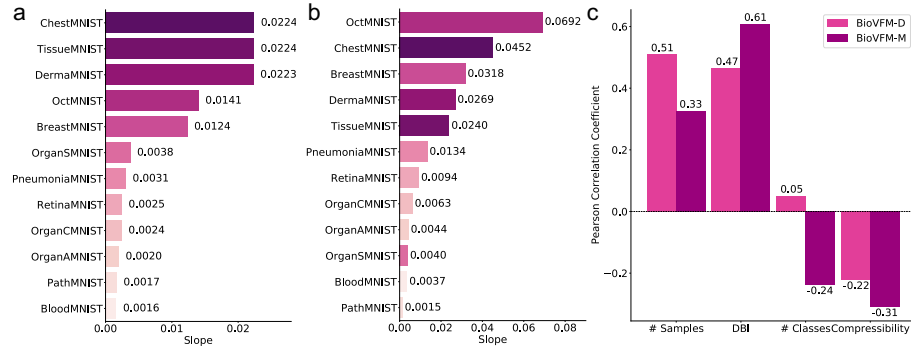


Fig. 4. Model scaling slopes and correlation to benchmark properties. a. The model scaling slopes of BioVFM-D with 12 medical benchmarks. **b.** The model scaling slopes of BioVFM-M with 12 medical benchmarks. The colors are consistent for each task. **c.** The Pearson correlation coefficient between model scaling slopes and benchmark metrics.

4.5 Correlations between benchmark properties and scaling slopes

To investigate the underlying impact factors related to scaling efficiency, we take model scaling as an example and perform a Pearson correlation coefficient analysis between quantitative metrics and scaling slopes. As shown in Figure 3c, the number of samples and DBI demonstrate a stronger correlation with model scaling slopes. A higher DBI indicates that the data has less distinct clusters, which increases the classification difficulty. This complexity necessitates larger models to capture complex decision boundaries, thus demonstrating better scaling efficiency. Additionally, the number of samples is positively correlated with model scaling slopes, as larger models can remember more information from more data to improve performance. Another meaningful indicator is g-zip compressibility, which measures the ratio of the compressed data size to the original size in bytes. Images with more redundancy will exhibit lower g-zip compressibility scores. Interestingly, we observed a negative correlation between g-zip compressibility and model scaling slopes, suggesting that larger models are more effective in handling image redundancy. In summary, larger models are advantageous for complex tasks, such as intricate decision boundaries and high data redundancy. However, simpler tasks should balance the diminishing returns of scaling with the associated computational overhead.

5 Discussion

This paper presents a systematic empirical study on the scalability of self-supervised learning for medical vision foundation models. We develop a large-scale medical image dataset to support this study. We investigate the scaling

behavior over model sizes, data sizes, image modalities, and pretraining algorithms. Our results reveal that while scaling up did demonstrate benefits for medical foundation models, several important factors including pretraining algorithm, data diversity, or task complexity contribute to the varied scaling behaviors. We believe that this study paves the way for future medical AI systems that can adapt to a wide range of clinical tasks and settings. Finally, we propose BioVFM, a medical vision foundation model at scale, demonstrating superior performance across 12 medical benchmarks. We will open the dataset, model, and algorithms of this study at <https://github.com/JiarunLiu/BioVFM>.

Acknowledgments. This research was partly supported by the National Natural Science Foundation of China (No. 62222118, No. U22A2040), Shenzhen Science and Technology Program (No. JCYJ20220531100213029), Shenzhen Medical Research Fund (No. B2402047), the Major Key Project of PCL under Grant PCL2024A06, National Key R&D Program of China (No. 2023YFA1011400), Key Laboratory for Magnetic Resonance and Multimodality Imaging of Guangdong Province (No. 2023B1212060052), and Youth Innovation Promotion Association CAS.

References

1. Alabdulmohsin, I.M., Zhai, X., Kolesnikov, A., Beyer, L.: Getting ViT in shape: Scaling laws for compute-optimal model design. In: *Advances in Neural Information Processing Systems*. vol. 36, pp. 16406–16425. Curran Associates, Inc. (2023)
2. Azad, B., et al.: Foundational models in medical imaging: A comprehensive survey and future vision. *arXiv preprint arXiv:2310.18689* (2023)
3. Butoi, V.I., Ortiz, J.J.G., Ma, T., Sabuncu, M.R., Guttag, J., Dalca, A.V.: Universeg: Universal medical image segmentation. In: *Proceedings of the IEEE/CVF International Conference on Computer Vision*. pp. 21438–21451 (2023)
4. Davies, D.L., Bouldin, D.W.: A cluster separation measure. *IEEE Transactions on Pattern Analysis and Machine Intelligence* **PAMI-1**(2), 224–227 (1979). <https://doi.org/10.1109/TPAMI.1979.4766909>
5. Hägele, A., Bakouch, E., Kosson, A., Allal, L.B., Von Werra, L., Jaggi, M.: Scaling laws and compute-optimal training beyond fixed training durations. *arXiv preprint arXiv:2405.18392* (2024)
6. He, K., Chen, X., Xie, S., Li, Y., Dollár, P., Girshick, R.: Masked autoencoders are scalable vision learners. In: *2022 IEEE/CVF Conference on Computer Vision and Pattern Recognition (CVPR)*. pp. 15979–15988 (2022). <https://doi.org/10.1109/CVPR52688.2022.01553>
7. Hoffmann, J., et al.: Training compute-optimal large language models. In: *Proceedings of the 36th International Conference on Neural Information Processing Systems*. NIPS '22, Curran Associates Inc., Red Hook, NY, USA (2022)
8. Huang, W., et al.: Enhancing representation in radiography-reports foundation model: A granular alignment algorithm using masked contrastive learning. *Nature Communications* **15**(1), 7620 (2024). <https://doi.org/10.1038/s41467-024-51749-0>
9. Huang, W., et al.: Enhancing the vision–language foundation model with key semantic knowledge-emphasized report refinement. *Medical Image Analysis* **97**, 103299 (2024). <https://doi.org/10.1016/j.media.2024.103299>

10. Jones, C., Castro, D.C., De Sousa Ribeiro, F., Oktay, O., McCradden, M., Glocker, B.: A causal perspective on dataset bias in machine learning for medical imaging. *Nature Machine Intelligence* **6**(2), 138–146 (2024). <https://doi.org/10.1038/s42256-024-00797-8>
11. Kaplan, J., et al.: Scaling laws for neural language models. arXiv preprint arXiv:2001.08361 (2020)
12. Lin, W., et al.: PMC-CLIP: Contrastive language-image pre-training using biomedical documents. In: *Medical Image Computing and Computer Assisted Intervention – MICCAI 2023*. vol. 14227, pp. 525–536. Springer Nature Switzerland (2023). https://doi.org/10.1007/978-3-031-43993-3_51
13. Liu, J., et al.: Swin-UMamba†: Adapting Mamba-based vision foundation models for medical image segmentation. *IEEE Transactions on Medical Imaging* pp. 1–1 (2024). <https://doi.org/10.1109/TMI.2024.3508698>
14. Liu, P., Puonti, O., Hu, X., Alexander, D.C., Iglesias, J.E.: Brain-id: Learning contrast-agnostic anatomical representations for brain imaging. In: *European Conference on Computer Vision*. pp. 322–340. Springer (2024)
15. Ma, J., He, Y., Li, F., Han, L., You, C., Wang, B.: Segment anything in medical images. *Nature Communications* **15**(1), 654 (2024). <https://doi.org/10.1038/s41467-024-44824-z>
16. Mei, X., et al.: RadImageNet: An open radiologic deep learning research dataset for effective transfer learning. *Radiology: Artificial Intelligence* **4**(5) (2022). <https://doi.org/10.1148/ryai.210315>
17. Moor, M., et al.: Foundation models for generalist medical artificial intelligence. *Nature* **616**(7956), 259–265 (2023). <https://doi.org/10.1038/s41586-023-05881-4>
18. Oquab, M., et al.: DINOv2: Learning robust visual features without supervision. *Transactions on Machine Learning Research* (2024)
19. Pandey, R.: gzip predicts data-dependent scaling laws. arXiv preprint arXiv:2405.16684 (2024)
20. Pérez-García, F., Sharma, H., Bond-Taylor, S., Bouzid, K., Salvatelli, V., Ilse, M., Bannur, S., Castro, D.C., Schwaighofer, A., Lungren, M.P., et al.: Exploring scalable medical image encoders beyond text supervision. *Nature Machine Intelligence* pp. 1–12 (2025). <https://doi.org/10.1038/s42256-024-00965-w>
21. Porian, T., Wortsman, M., Jitsev, J., Schmidt, L., Carmon, Y.: Resolving discrepancies in compute-optimal scaling of language models. In: *The Thirty-eighth Annual Conference on Neural Information Processing Systems* (2024)
22. Vorontsov, E., et al.: A foundation model for clinical-grade computational pathology and rare cancers detection. *Nature medicine* **30**(10), 2924–2935 (2024). <https://doi.org/10.1038/s41591-024-03141-0>
23. Wang, S., et al.: Annotation-efficient deep learning for automatic medical image segmentation. *Nature communications* **12**(1), 5915 (2021). <https://doi.org/10.1038/s41467-021-26216-9>
24. Yang, H., et al.: Multi-modal vision-language model for generalizable annotation-free pathology localization and clinical diagnosis. arXiv preprint arXiv:2401.02044 (2024)
25. Yang, J., et al.: MedMNIST v2 - a large-scale lightweight benchmark for 2D and 3D biomedical image classification. *Scientific Data* **10**, 41 (2023). <https://doi.org/10.1038/s41597-022-01721-8>
26. Zhai, X., Kolesnikov, A., Houlsby, N., Beyer, L.: Scaling vision transformers. In: *2022 IEEE/CVF Conference on Computer Vision and Pattern Recogni-*

- tion (CVPR). pp. 1204–1213 (2022). <https://doi.org/10.1109/CVPR52688.2022.01179>
27. Zhang, K., et al.: A generalist vision–language foundation model for diverse biomedical tasks. *Nature Medicine* **30**, 3129–3141 (2024). <https://doi.org/10.1038/s41591-024-03185-2>
 28. Zhang, S., Metaxas, D.: On the challenges and perspectives of foundation models for medical image analysis. *Medical Image Analysis* **91**, 102996 (2024). <https://doi.org/10.1016/j.media.2023.102996>
 29. Zhang, S., et al.: BiomedCLIP: a multimodal biomedical foundation model pretrained from fifteen million scientific image-text pairs. arXiv preprint arXiv:2303.00915 (2023)
 30. Zhou, H.Y., Chen, X., Zhang, Y., Luo, R., Wang, L., Yu, Y.: Generalized radiograph representation learning via cross-supervision between images and free-text radiology reports. *Nature Machine Intelligence* **4**(1), 32–40 (2022). <https://doi.org/10.1038/s42256-021-00425-9>
 31. Zhou, H.Y., Lu, C., Chen, C., Yang, S., Yu, Y.: A unified visual information preservation framework for self-supervised pre-training in medical image analysis. *IEEE Transactions on Pattern Analysis and Machine Intelligence* **45**(7), 8020–8035 (2023). <https://doi.org/10.1109/TPAMI.2023.3234002>
 32. Zhou, H.Y., et al.: A transformer-based representation-learning model with unified processing of multimodal input for clinical diagnostics. *Nature biomedical engineering* **7**(6), 743–755 (2023). <https://doi.org/10.1038/s41551-023-01045-x>
 33. Zhou, Y., et al.: A foundation model for generalizable disease detection from retinal images. *Nature* **622**(7981), 156–163 (2023). <https://doi.org/10.1038/s41586-023-06555-x>